Measurement of the band offsets of SiO_2 on clean *n*- and *p*-type GaN(0001)

T. E. Cook, Jr., C. C. Fulton, W. J. Mecouch, K. M. Tracy, and R. F. Davis
Department of Materials Science and Engineering, North Carolina State University, Raleigh, North Carolina 27695

E. H. Hurt, G. Lucovsky, and R. J. Nemanich
Department of Physics, North Carolina State University, Raleigh, North Carolina 27695-8202

(Received 4 November 2002; accepted 16 January 2003)

The band alignment at the SiO_2-GaN interface is important for passivation of high voltage devices and for gate insulator applications. X-ray photoelectron spectroscopy and ultraviolet photoemission spectroscopy have been used to observe the interface electronic states as SiO_2 was deposited on clean GaN(0001) surfaces. The substrates, grown by metallorganic chemical vapor deposition, were *n*- (1×10^{17}) and *p*-type (2×10^{18}) GaN on 6*H*-SiC(0001) with an AlN(0001) buffer layer. The GaN surfaces were atomically cleaned via an 860 °C anneal in an NH_3 atmosphere. For the clean surfaces, *n*-type GaN showed upward band bending of 0.3 ± 0.1 eV, while *p*-type GaN showed downward band bending of 1.3 ± 0.1 eV. The electron affinity for *n*- and *p*-type GaN was measured to be 2.9 ± 0.1 and 3.2 ± 0.1 eV, respectively. To avoid oxidizing the GaN, layers of Si were deposited on the clean GaN surface via ultrahigh vacuum *e*-beam deposition, and the Si was oxidized at 300 °C by a remote O_2 plasma. The substrates were annealed at 650 °C for densification of the SiO_2 films. Surface analysis techniques were performed after each step in the process, and yielded a valence band offset of 2.0 ± 0.2 eV and a conduction band offset of 3.6 ± 0.2 eV for the GaN-SiO_2 interface for both *p*- and *n*-type samples. Interface dipoles of 1.8 and 1.5 eV were deduced for the GaN-SiO_2 interface for the *n*- and *p*-type surfaces, respectively. © *2003 American Institute of Physics.* [DOI: 10.1063/1.1559424]

I. INTRODUCTION

Gallium nitride is being investigated for a wide range of electronic and optoelectronic applications. In particular, the interfacial band alignment is of significant interest in the fabrication of devices based on heterostructures. The heterojunction band discontinuities are key parameters of device design because the valence and conduction band offsets determine the transport and confinement properties at the interface. A fundamental objective for technology and basic research would be the control of the band discontinuities.[1] The deposition of SiO_2 on GaN could be important for passivation of high-voltage devices and for the gate insulator in field effect transistor devices.[2] While the Si-SiO_2 interface has been studied extensively,[3–7] little research has been reported and large uncertainties exist on the band offsets at nitride interfaces.[8–12]

Surface preparation is a critical step in controlled heterostructure formation. In prior studies Bermudez[13] compared GaN surfaces prepared by sputtering with nitrogen ions followed by annealing in ultrahigh vacuum (UHV) and surfaces prepared by *in situ* deposition of Ga metal followed by thermal desorption. For the two processes, no significant differences of the values of work function, band bending, and Ga 3*d* binding energy were found, which suggests that nitrogen-ion sputtering and annealing are equivalent for preparation of ordered GaN surfaces. However, surfaces prepared by these methods show additional emission at energies above the valence band maximum (VBM) in photoemission data that has been attributed to surface states. In our study, GaN is prepared by an *in situ* ammonia exposure at an elevated temperature,[14] producing atomically clean surfaces without observable emission above the VB turn-on.

Several groups have reported the electrical characteristics of the SiO_2-GaN interface grown by plasma enhanced chemical vapor deposition. Casey *et al.*[15] found no observable hysteresis in room temperature *C-V* measurements, as well as an increase of capacitance with incident ultraviolet light while in deep depletion. These observations are consistent with a low concentration of interface traps. M. Sawada *et al.*[16] and Arulkumaran *et al.*[17] support this observation, measuring $(1-2)\times10^{11}$ and 2.5×10^{11} cm^{-2} eV^{-1}, respectively, for the minimum interface state density at the SiO_2-GaN interface. T. Sawada *et al.*[18] investigated the effect of thermal annealing of the interface. The interface state density was reduced by 33% to 2×10^{11} cm^{-2} eV^{-1} after annealing in H_2 at 500 °C. Also noted was that the Fermi level was not pinned and could move within the upper band gap. The as-deposited sample had a Fermi level 0.2 eV from the conduction band edge under thermal equilibrium conditions, and the value increased to 0.5 eV after annealing. The relatively low interface trap density suggests the promise of applications for this interface. While several studies[19–21] have employed photoemission techniques to explore metal/GaN interfaces, there has been, to our knowledge, no similar report for the SiO_2-GaN interface.

An approach to describing a heterostructure interface is to apply the electron affinity model (EAM). This model holds in the ideal case, assuming there is no potential created as the heterostructure is formed. The alternative model is the

interface dipole model, where the structure of the interface causes a shift in the entire band lineup relative to the predictions of the EAM. The well-known occurrence of reconstructions, chemical reactions, dislocations and strain at the interface may result in contributions to the so-called structural interface dipole.[22] The focus of our experiment is to measure the band offsets and to compare the results to this dipole at the heterostructure interface.

The charge neutrality level (CNL) model has been used to describe the band alignment of a heterojunction interface between two semiconductors. Tersoff[23] suggested that the band alignment between two semiconductors is controlled by the charge transfer across the interface and the resulting interface dipoles in a fashion similar to Schottky barrier models. Recently, Robertson[24] employed the S parameter, which reflects the dielectric screening, to relate the relative contribution of the electron affinity model and the dipole from the charge neutrality levels. In this study, the correlation between the CNL model and experimental data will be presented.

In this study, *in situ* x-ray photoelectron spectroscopy (XPS) and ultraviolet photoemission spectroscopy (UPS) measurements are used to determine the band discontinuities, or band offsets, at the GaN-SiO_2 interface. This process is a well-established method that has been reported in the literature.[22,25,26] After achieving an atomically clean GaN(0001) surface, care is taken to avoid oxidation during the process. Our basic approach in this study is to obtain a clean GaN surface through an ammonia exposure at an elevated temperature and to form a SiO_2 layer by depositing silicon and to employ low temperature oxidation to minimize disruption of the interface. XPS and UPS measurements are obtained after each step of the process, and the band bending is deduced from the shifts of the gallium and nitrogen core levels. The band offsets and electron affinities are determined from the UPS spectra, and the formation of the oxide and the value of the interfacial dipole are determined from the XPS and UPS measurements.

II. EXPERIMENTAL PROCEDURES

The GaN films used in this study were grown via metallorganic chemical vapor deposition (MOCVD) on 50 mm diameter on-axis Si-face, 6H-SiC(0001) substrates with a conducting AlN(0001) buffer layer. The thicknesses of the GaN epilayer and the AlN buffer were 1.1 and 0.1 μm, respectively. Prior research has established that MOCVD growth of GaN on Si-face SiC(0001) results in Ga-face GaN(0001).[27,28] Silicon was used as the *n* dopant, and magnesium was used as the *p* dopant. Dopant concentrations (N_d-N_a) of 1×10^{17} and (N_a-N_d) of 2×10^{18} cm^{-3} were measured for the *n*- and *p*-type samples using capacitance-voltage measurements with a mercury probe.

Raman spectroscopy was employed to characterize the residual strain in the GaN film. The E_2 mode, which is employed to characterize the biaxial strain,[29] was found at 564.4 cm^{-1}. The E_2 mode is found at 567.2 cm^{-1} for a free standing film, and this value is used as the reference. Therefore, we deduce a residual tensile strain of 1.4×10^{-3} and a residual tensile stress of 0.6 GPa.[30]

Ex situ preparation of the GaN consisted of a process where the films were cleaned sequentially in trichloroethylene, acetone, and methanol baths for 1 min each, followed by immersion into 49% HCl for 10 min. The samples were then rinsed for 10 s in deionized water, and blown dry using nitrogen. The samples were mounted to molybdenum plates, secured by tantalum wires, and then placed in the load lock for entry into the transfer line that interconnects several analysis and processing chambers. The total time between the completion of *ex situ* cleaning and inserting into the system was about 10 min.

Initial surface analysis was performed, and the sample was moved to the gas source molecular beam epitaxy chamber for *in situ* cleaning. The cleaning process consists of annealing at 860 °C for 15 min in an NH_3 atmosphere. Ammonia was introduced into the chamber when the temperature reached 500 °C via a needle valve and a chamber pressure of 1×10^{-4} torr was obtained. The distance between the ammonia doser and sample was ~5 cm, and the partial pressure of ammonia at the sample surface is expected to be as much as an order of magnitude higher than the system pressure. After allowing 5 min for the pressure to stabilize, the heater was ramped to 860 °C at a rate of 30 °C per min. The temperature and ammonia flow were maintained for 15 min. Subsequently, a ramp rate of -40 °C per min^{-1} was used to achieve a heater temperature of 500 °C; the sample was held at this temperature while the needle valve was closed. The pressure decreased to the low 10^{-8} torr range, during which the sample cooled to ~200 °C, and was transferred out of the system.

After cleaning and other process steps, the samples were transferred in UHV for surface analysis. For XPS, a dual anode x-ray source was used to generate magnesium (1253.6 eV) or aluminum (1486.6 eV) x-rays, and the photoemitted electrons were analyzed with a Fisons Clam II. The resolution of the analyzer was determined from the full width at half maximum (FWHM) of a gold $4f_{7/2}$ spectral peak to be ~1.0 eV; however through curve fitting, spectral peak positions could be determined to ±1.0 eV. UPS with He *I* (21.2 eV) radiation was employed to measure the electronic states near the valence band and to determine the electron affinity. The photoemitted electrons were analyzed with a VSW 50 mm mean radius hemispherical analyzer operated with a resolution of 0.1 eV. A negative 4 V bias was applied to the sample to overcome the work function of the analyzer.

The XPS and UPS spectra were obtained after each process step in a sequence of experiments to follow the shifts of the XPS peaks and the evolution of the valence band spectra. The spectra were measured to track the peak shifts and discern the band bending and band offsets after each of the following steps: 2 Å Si deposition, a second 2 Å Si deposition (4 Å total), O_2 plasma at 300 °C, 2 Å Si (6 Å total Si) and O_2 plasma at 300 °C, 650 °C anneal for 15 min, a final 3 Å Si deposition (9 Å Si total) and O_2 plasma at 300 °C, and a 15 min 650 °C final anneal. Throughout the manuscript, references to the Si thickness in the processing steps refer to the total amount of Si deposited up to that particular step. The ultimate thickness of the oxide film was calculated to be ~18 Å using a density comparison method. This thickness

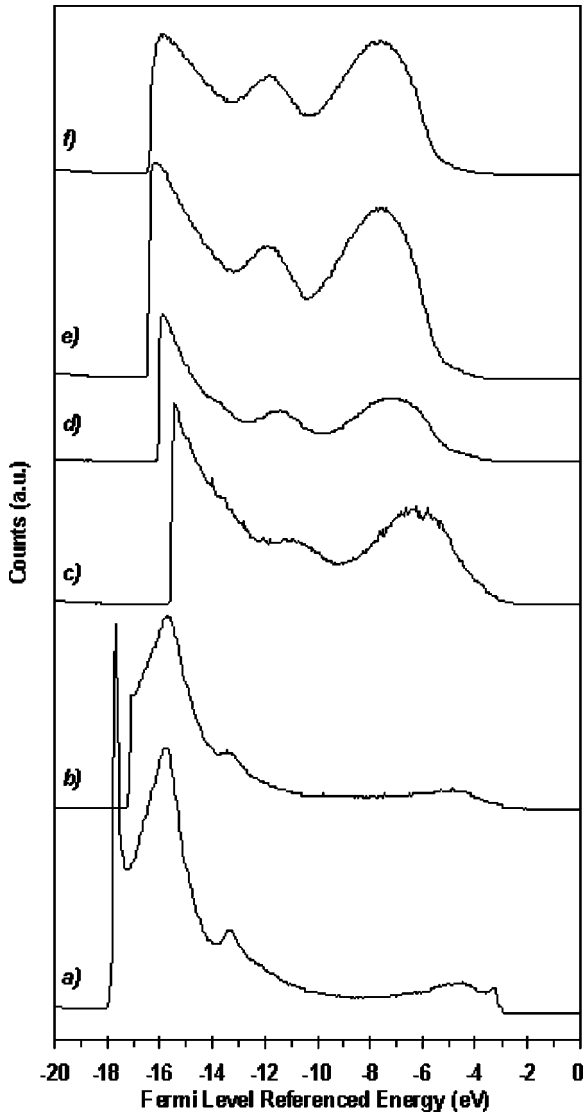

FIG. 1. UPS spectra of (a) CVC *n*-type GaN, (b) 2 Å Si, (c) 4 Å Si and O_2 plasma, (d) 6 Å Si, O_2 plasma, and 650 °C anneal, (e) 9 Å Si and O_2 plasma, and (f) 650 °C anneal.

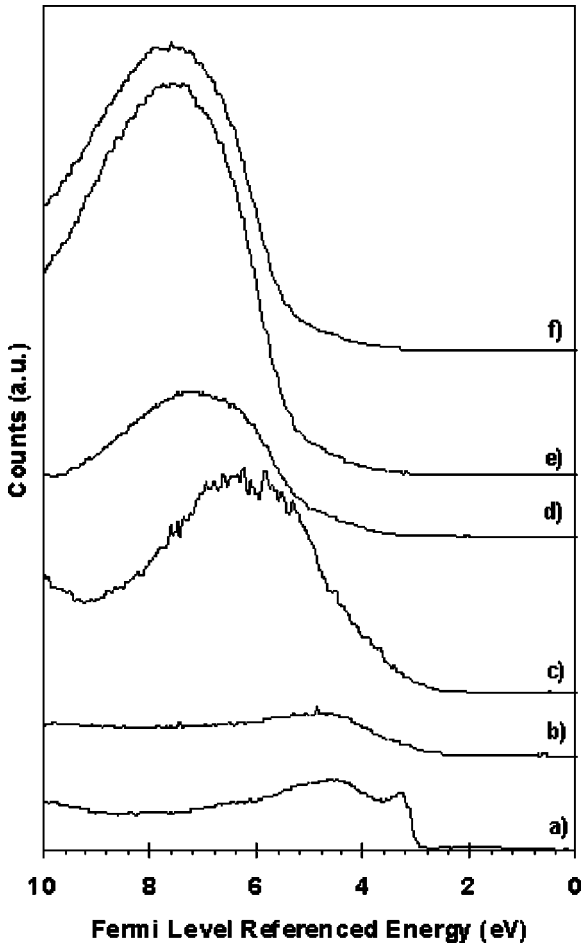

FIG. 2. UPS spectra of the valence band maximum of (a) CVC *n*-type GaN, (b) 2 Å Si, (c) 4 Å Si and O_2 plasma, (d) 6 Å Si, O_2 plasma and 650 °C anneal, (e) 9 Å Si and O_2 plasma, and (f) 650 °C anneal.

was measured experimentally to be ~17 Å by examining the XPS core level intensities for the clean and final process steps.

III. RESULTS

The evolution of the UPS spectra from the clean GaN through oxidation and anneal of the deposited 9 Å Si for the *n*-type experiment is shown in Figs. 1 and 2. The VBM of the clean GaN surface was determined from an extrapolation of a line fit to the leading edge of the spectrum. A turn-on of the GaN signal was measured at 3.0 ± 0.1 eV (referenced to the Fermi level). From the doping concentration of 1×10^{17} in the GaN, the bulk Fermi level was determined to be ~100m eV below the conduction band minimum. Because the deposited layers obscure the valence band maximum, in order to follow the position of the VBM, it is necessary to detect a more intense bulk GaN spectral feature to reference the position of the VBM. A feature at 13.4 eV in the spectra shown in Fig. 1 has been attributed to a GaN bulk excitation.[31] Note that this feature shifts to a higher binding energy by 0.3 ± 0.1 eV with the deposition of 4 Å of Si and the oxidation that followed. This shift is an indication of a reduction of the band bending by 0.3 eV and is consistent with essentially flatband conditions after the oxidation. Tracking the peak movement is only possible when the substrate emission is observable; therefore when the layer thickness obscures this emission, no further information can be obtained. In our UPS measurements, emission from the substrate was not detected for the 9 Å silicon deposition and oxidation. With increased thickness, the turn-on and signature peaks for SiO_2 remained unchanged.

The spectra shown in Fig. 1 were used to determine the electron affinity of GaN, as well as the deposited SiO_2. The electron affinity can be determined by the relation

$$\chi = h\nu - W - E_g, \tag{1}$$

where W is the spectral width from the VBM to the low energy cutoff, $h\nu$ is the photon energy (21.2 eV), and E_g is the band gap of the material. For different cleaning procedures the VBM is sometimes obscured by surface states,[13,32] but for this study we will employ the method noted above, assuming it is representative of the VBM. For the clean GaN surface, the width of the spectrum was measured to be 14.9 and 14.6 eV for the *n*- and *p*-type surface, respectively. Us-

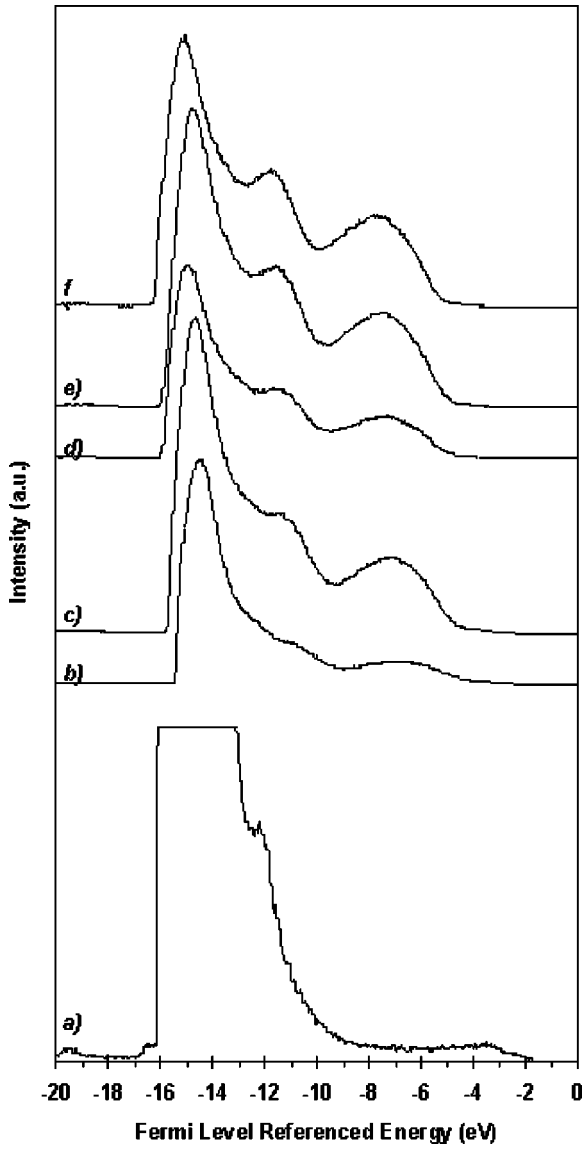

FIG. 3. UPS spectra of the valence band maximum of (a) CVC *p*-type GaN, (b) 4 Å Si and O_2 plasma, (c) 6 Å Si and O_2 plasma, (d) 6 Å Si, O_2 plasma, and 650 °C anneal, (e) 9 Å Si and O_2 plasma, (f) 650 °C final anneal.

ing the generally accepted band gap of GaN, 3.4 eV, the electron affinity was determined to be 2.9 and 3.2 eV for the *n*- and *p*-type surface, respectively. While the electron affinity differs by 0.3 eV between the two samples, this is within the experimental error and in agreement with prior reports of 3.0 eV for GaN.[13,20,33]

We employ the same approach to determine the electron affinity of the SiO_2 layer. The turn-on for the SiO_2 is observed at ~5.1 eV below the Fermi level, and the spectral width is measured to be 11.1 eV. Assuming a bandgap of 9.0 eV, we obtain an electron affinity of 1.1 eV, which is consistent with prior reports.[24]

The scans shown in Fig. 3 represent the evolution of the UPS spectra from the clean GaN through the final surface for the *p*-type substrate. Figure 4 presents an expanded scan of the clean surface, which indicates a VBM at 1.6 eV (referenced to the Fermi level). Based on the 2×10^{18} cm^{-3} doping of the Mg, the bulk Fermi level is calculated to be

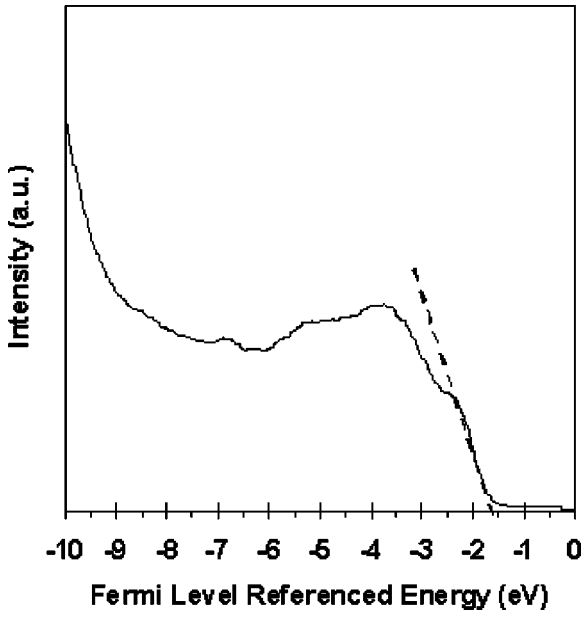

FIG. 4. UPS spectra of the valence band maximum of CVC *p*-type GaN, with valence band maximum indicated by a dashed line.

~300m eV above the VBM. The GaN bulk feature observed at 12.2 eV is in agreement with values reported elsewhere.[19] This feature shifts to a higher binding energy by 0.9 ± 0.1 eV with the formation of the SiO_2 layer.

The evolution of the gallium 3*d* peak during the *n*-type GaN experiment is shown in Fig. 5. The initial peak position and width of the peak for the clean surface were determined to be 20.4 ± 0.1 and 1.35 ± 0.1 eV, respectively. This peak position minus the VB turn-on is 17.4 eV, and is close to the value of 17.7 eV reported by Waldrop and Grant.[34] In some data sets we have found values consistent with the 17.7 eV

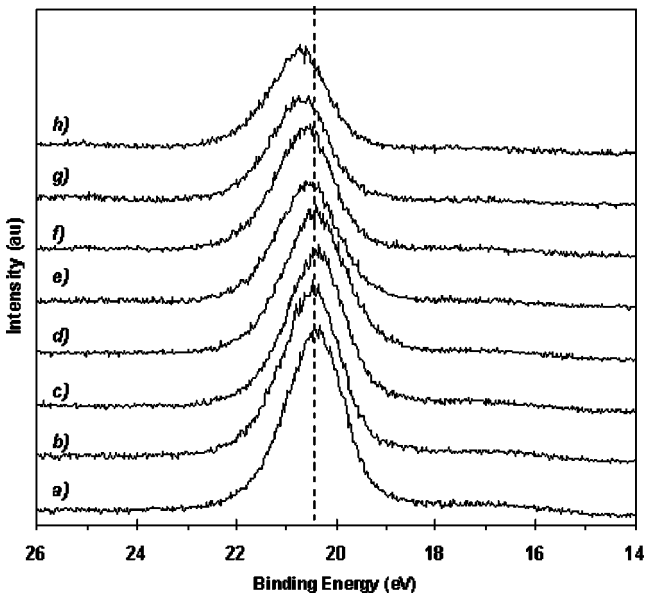

FIG. 5. Gallium 3*d* XPS spectra for (a) CVC *n*-type GaN, (b) 2 Å Si deposition, (c) 4 Å Si deposition, (d) 4 Å Si and O_2 plasma, (e) 6 Å Si, O_2 plasma, (f) 6 Å Si, O_2 plasma, and 650 °C anneal, (g) 9 Å Si and O_2 plasma, and (h) 650 °C final anneal. The peak positions of the initial surface as well as the final surface are indicated with dashed lines.

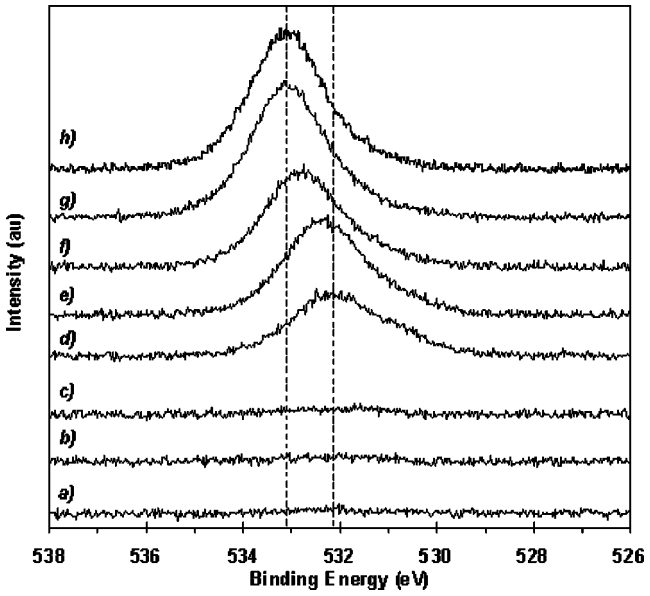

FIG. 6. Oxygen 1s XPS spectra for (a) CVC *n*-type GaN, (b) 2 Å Si deposition, (c) 4 Å Si deposition, (d) 4 Å Si and O_2 plasma, (e) 6 Å Si, O_2 plasma, (f) 6 Å Si, O_2 plasma, and 650 °C anneal, (g) 9 Å Si and O_2 plasma, and (h) 650 °C final anneal. The peak positions after the initial oxidation as well as the final surface are indicated with dashed lines.

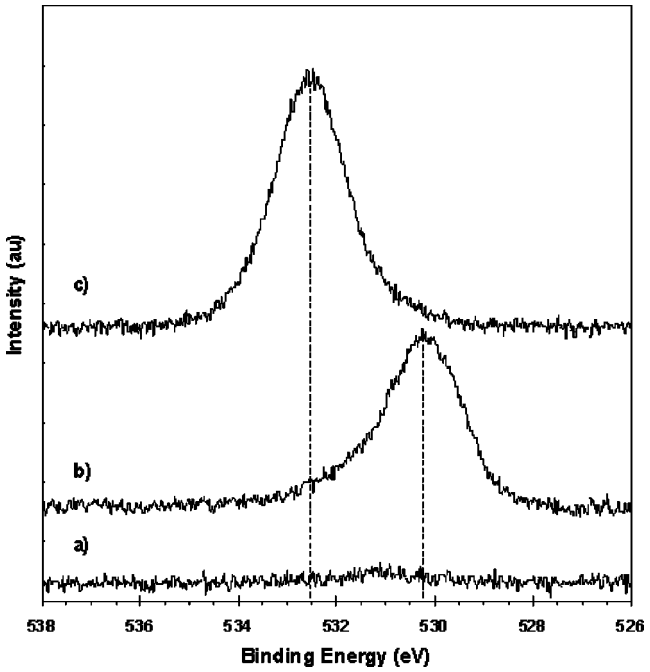

FIG. 7. Oxygen 1*s* XPS spectra for (a) CVC *p*-GaN, (b) O_2 plasma, and (c) final SiO_2 surface. Dashed lines indicate the peak positions for the oxidized GaN as well as the final SiO_2 surface.

found by Waldrop and Grant.[34] In our case the core level and valence band measurements are made with two separate instruments and variations in calibration are likely responsible for the small differences. The primary considerations of our measurements are about relative peak shifts, so these small variations do not affect our analysis.

Spectra observed after the first and second 2 Å Si depositions showed shifts that were smaller than 0.1 eV. After an anneal following the third 2 Å Si deposition (6 Å total) and oxidation, the peak shifted to 20.65 ± 0.1 eV, while the width increased to 1.4 ± 0.1 eV. For the final surface, which consisted of a 9 Å Si layer that was oxidized, the peak was observed at 20.76 ± 0.1 eV, indicating a shift of 0.36 ± 0.1 eV for the entire experiment. There are no indications of a reaction between the GaN and the SiO_2, therefore suggesting that this shift is due to a change in the band bending.[35]

Similar behavior was observed for the evolution of the nitrogen 1s core level. The N 1s peak position for the clean *n*-type GaN surface was observed at 397.9 ± 0.1 eV, and the width was measured to be 1.1 ± 0.1 eV. As in the case of the Ga 3*d*, the N 1s shifted a discernible amount after the third 2 Å Si deposition (6 Å total) and oxidation, to 398.2 ± 0.1 eV, with a width of 1.2 ± 0.1 eV. For the final surface, the peak shifted to 398.3 ± 0.1 eV, with a width of 1.1 ± 0.1 eV. This difference of 0.37 ± 0.1 eV is again consistent with values obtained for the gallium core level peaks.

Figure 6 displays the evolution of the oxygen 1s core level. As measured by XPS, the as-loaded GaN sample contains ~14 and 8 at. % of oxygen and carbon, respectively. The chemical vapor clean (CVC) reduces the oxygen and carbon below the XPS detection limits (<1 at. %).

The surface termination of the GaN after the CVC has not been determined. The Si 2*p* and N 1s core levels were examined for evidence of Si-N bonding immediately after the first silicon deposition. For the Si 2*p*, the nearby location of the Ga 3*p* core level, as well as the subtle difference in peak location for Si-O and Si-N bonding limited the ability to detect Si-N bonding. Similarly, we found that the N 1s core levels in GaN and in Si_3N_4 deposited on GaN essentially overlap. With these considerations, we cannot exclude the possibility of Si-N at the surface even though no direct evidence was found in our measurements.

After deposition of 4 Å Si and the O_2 plasma, the initial peak position was observed at 532.2 ± 0.1 eV. Through the course of the experiment, the peak shifted to 533.1 eV, for a total of 0.9 ± 0.1 eV. This peak only slightly deviates by 0.2 eV from the 533.3 eV value reported in the literature for SiO_2 on silicon substrates.[36,37] The final peak position for the O 1s core level of the SiO_2 on *p*-type GaN is at 532.5 eV, which is also generally consistent with the prior value.

The oxide quality is an important issue because it affects the band gap of the material. Careful comparisons were made of the oxide grown on the GaN surface with SiO_2 grown on silicon. The difference in energy between the O 1*s* and Si 2*p* core levels was found to be 429.5 eV in the oxide grown in our experiment, which is equivalent to the value found in the literature.[38] This finding suggests that the quality of our film is consistent with SiO_2 grown on Si.

Figure 7 shows the O 1*s* core level for *p*-type GaN CV cleaned, oxidized, and SiO_2 surfaces. The oxidized GaN surface has a peak position of 530.2 eV. The SiO_2 surface shown is that of the final surface of the *p*-type experiment, and has a peak position of 532.5 eV. The Ga-O bond found in the oxidized case could not be resolved in the SiO_2 spectra. The Ga 3*p* core level has a higher surface sensitivity than the Ga 3*d* core level, and is shown in Tables I and II for the n- and *p*-type experiments. The Ga 3*p* core level displays shifts

TABLE I. XPS core level curve fitting results for the *n*-type GaN experiment. (Oxygen plasma is represented as O-Pl.)

	Ga $3p_{3/2}$		Si 2*p*		O 1s		Ga 3*d*		N 1s	
Process step	Center (eV)	FWHM (eV)	Center (eV)	FWHM (eV)	Center (eV)	FWHM (eV)	Center (eV)	FWHM (eV)	Center (eV)	FWHM (eV)
CVC	105.71	2.69	—	—	—	—	20.41	1.35	397.90	1.10
2 Å Si	105.71	2.67	101.59	3.72	—	—	20.48	1.35	398.02	1.12
4 Å Si	105.71	2.68	100.90	2.87	—	—	20.46	1.35	398.01	1.13
O-Pl	105.73	2.66	102.71	2.26	532.19	1.94	20.45	1.40	398.01	1.29
6 Å Si, O-Pl	105.89	2.68	102.95	2.06	532.37	1.85	20.56	1.44	398.05	1.26
Anneal	106.01	2.65	103.54	2.15	532.81	1.76	20.65	1.41	398.16	1.14
9 Å Si, O-Pl	106.03	2.68	103.59	1.92	533.10	1.77	20.74	1.37	398.25	1.11
Final	106.10	2.54	103.61	1.98	533.10	1.77	20.76	1.37	398.27	1.14
Difference	0.39		2.02		0.91		0.35		0.37	

that are consistent with those of the Ga 3*d* and N 1s core levels, without indication of a chemical shift due to Ga_2O_3 formation. As mentioned previously, the SiO_2 formed on the surface is shown to have a limited reaction with the GaN and is below the detection limits in XPS.

Further evidence of SiO_2 formation can be detected in the silicon 2*p* peak spectra. After Si deposition, the initial peak position was observed at 101.59 ± 0.1 eV. This peak shifted to 103.61 ± 0.1 eV after oxidation and subsequent annealing of the substrate. This peak position, as well as the shift of 2 eV, is consistent with SiO_2 on Si substrates,[39] which we attribute to a chemical shift due to the formation of SiO_2 .

The evolution of the gallium 3*d* peak for the *p*-type GaN experiment is shown in Fig. 8. The initial peak position for the clean surface was observed at 19.18 ± 0.1 eV. After the 4 Å Si deposition and oxidation, the peak shifted to a value of 19.4 ± 0.1 eV. While the peak shifted ~ 0.2 eV during the oxidation, the largest shift occurred after each anneal of the sample, as evidenced by the peak positions of the 6 Å total Si/O_2 plasma/650 °C anneal and the 9 Å total Si/O_2 plasma/650 °C anneal treatments shown at 19.95 ± 0.1 and 20.05 ± 0.1 eV, respectively. Annealing is a well-documented process for densification of the deposited oxide, which enhances the quality of the film.[40–42] During the course of the experiment we observed a shift in the spectra of 0.87 ± 0.1 eV. The lack of a Ga-O peak in the spectra once again suggests a very limited reaction between the GaN and the SiO_2, implying that this shift is due to a change in the band bending.

The peak position of the nitrogen 1s core level on the clean *p*-type GaN surface was observed at 396.65 ± 0.1 eV, while the final position was 397.5 ± 0.1 eV. This difference of 0.85 ± 0.1 eV is in excellent agreement with values for the Ga 3*d* levels.

The spectral peak positions and the FWHM for Ga $3p_{3/2}$, Si 2*p*, O 1*s*, Ga 3*d*, and N 1*s* have been summarized in Tables I and II for both *n*- and *p*-type GaN, respectively. From the results, two important properties of the interface can be stated. First, there does not appear to be a significant reaction at the GaN-SiO_2 interface. If this reaction were significant, there would be additional peaks reflecting the reacted environment, and/or changes in the widths of the peaks. Second, the observed shift for the Ga $3p_{3/2}$, Ga 3*d*, and N 1*s* core levels are essentially the same, allowing the inference that the shifts are a result of band bending.

IV. DISCUSSION

The method for determining the valence band discontinuity is similar to that of Waldrop and Grant[34] and Kraut *et al.*[43] Their basic approach is to reference the VBM to a core level in the XPS spectrum for each semiconductor and to use the measured difference between the core level energies to discern the band discontinuities. In our study, we have employed UPS to measure the energy of the VBM from the Fermi level, and XPS is used to measure core level energies relative to the Fermi level.

Care was taken to avoid oxidation of the clean GaN surface after the CVC. A significant Ga_2O_3 layer at the interface can be a source of deep acceptors and interface states that can be detrimental to device fabrication.[44] Although gallium oxide was not observed within our detection limits, we

TABLE II. XPS core level curve fitting results for the *p*-type GaN experiment.

	Ga $3p_{3/2}$		Si 2*p*		O 1s		Ga 3*d*		N 1s	
Process step	Center (eV)	FWHM (eV)	Center (eV)	FWHM (eV)	Center (eV)	FWHM (eV)	Center (eV)	FWHM (eV)	Center (eV)	FWHM (eV)
CVC	104.53	2.81	—	—	—	—	19.18	1.64	396.65	1.34
4 Å Si	104.8	2.91	99.8	3.81	531.34	2.57	19.55	1.66	396.93	1.31
O-Pl	104.74	2.51	102.42	2.45	531.83	2.02	19.4	1.61	396.8	1.33
6 Å Si, O-Pl	104.86	2.70	102.84	2.46	531.94	1.92	19.42	1.63	396.82	1.36
Anneal	105.37	2.77	103.3	1.74	532.36	1.58	19.95	1.66	397.35	1.37
9 Å Si, O-Pl	104.72	2.98	102.68	1.90	532.0	1.80	19.48	1.61	396.9	1.27
Final	105.41	2.85	103.34	1.95	532.53	1.52	20.05	1.72	397.5	1.36
Difference	0.88		3.54		1.19		0.87		0.85	

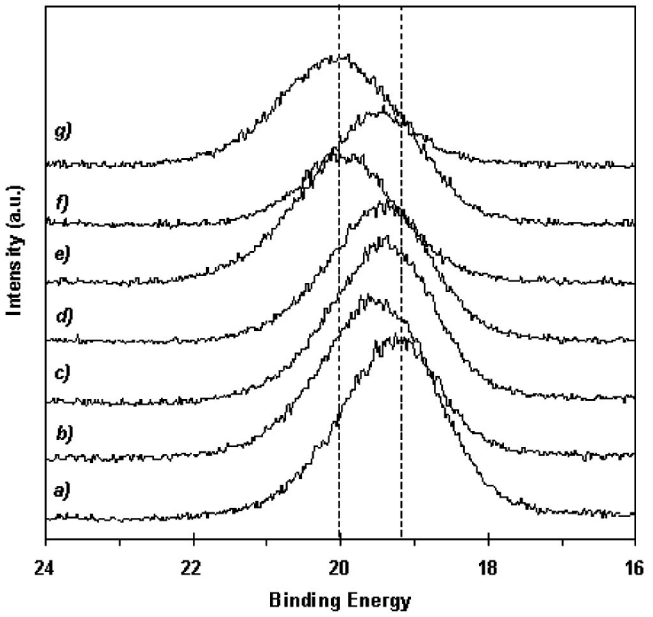

FIG. 8. Gallium 3*d* XPS spectra for (a) CVC *p*-type GaN, (b) 4 Å Si deposition, (c) 4 Å Si and O_2 plasma, (d) 6 Å Si, O_2 plasma, (e) 6 Å Si, O_2 plasma, and 650 °C anneal, (f) 9 Å Si and O_2 plasma, and (g) 650 °C final anneal. The peak positions of the initial surface as well as the final surface are indicated with dashed lines.

expect that Ga-O bonding exists at the SiO_2-GaN interface. Therrien *et al.*[45] reported the significance of an ultrathin Ga_2O_3 layer formation, which allowed a redistribution of electronic charge and reduction of the interfacial defect density.

The Ga-face GaN(0001) is a polar surface, and the spontaneous polarization will lead to a negative bound charge at the GaN film surface and a positive bound charge at the back substrate interface. The GaN is also piezoelectric, but because the films are grown above the critical thickness there is only a small residual strain, and the piezoelectric induced polarization ($P_{pz}=0.002$ C/m^2) is small in comparison to the spontaneous polarization ($Psp=0.033$ C/m^2).[46] The piezoelectric polarization for biaxial tensile strain contributes in the same direction as the spontaneous polarization. The negative surface bound charge is compensated by surface states and screened by ionized donors while the positive bound charge at the substrate interface is screened by the free carriers. The polarization bound charge screened by the ionized donors would lead to upward band bending at the GaN surface. We note that the XPS measurements of the Ga and N core levels would be shifted by the polarization fields, but all measurements of the band offsets are made relative to these values, and thus the measured band offsets should not be affected by polarization induced band bending. Moreover, since the strain is relatively small, the effect of strain on the band offsets is anticipated to be less than the experimental uncertainties in our measurements.[47]

Figure 9 shows the proposed band lineups for the *n*-type GaN-SiO_2 interface. The decrease of 0.3 eV band bending from the clean surface indicates that essentially flatband conditions are achieved. The valence band offset determination is the measured UPS turn-on for SiO_2 (5.3 eV), minus the GaN turn-on (3.0 eV), minus the band bending (0.3 eV). With this value and the knowledge of the band gap of the material, the conduction band offset is obtained. The band gap of SiO_2 has been widely reported to be 9.0 eV,[48–50] and this value was used for the conduction band offset and electron affinity calculations. From our experiment, the valence band offset is deduced to be 2.0 eV, and the conduction band offset is 3.6 eV.

The *p*-type GaN-SiO_2 band lineup is represented in Fig. 10. For the clean surface, the measured downward band bending and electron affinity were calculated to be 1.3 ± 0.1 and 3.2 ± 0.1 eV, respectively, assuming that the Mg acceptor level lies ~300 meV above the VBM and that the room temperature band gap is 3.4 eV.[51] Using the considerations mentioned above, the valence band offset was calculated to be 2.0 eV, and the conduction band offset of 3.6 eV.

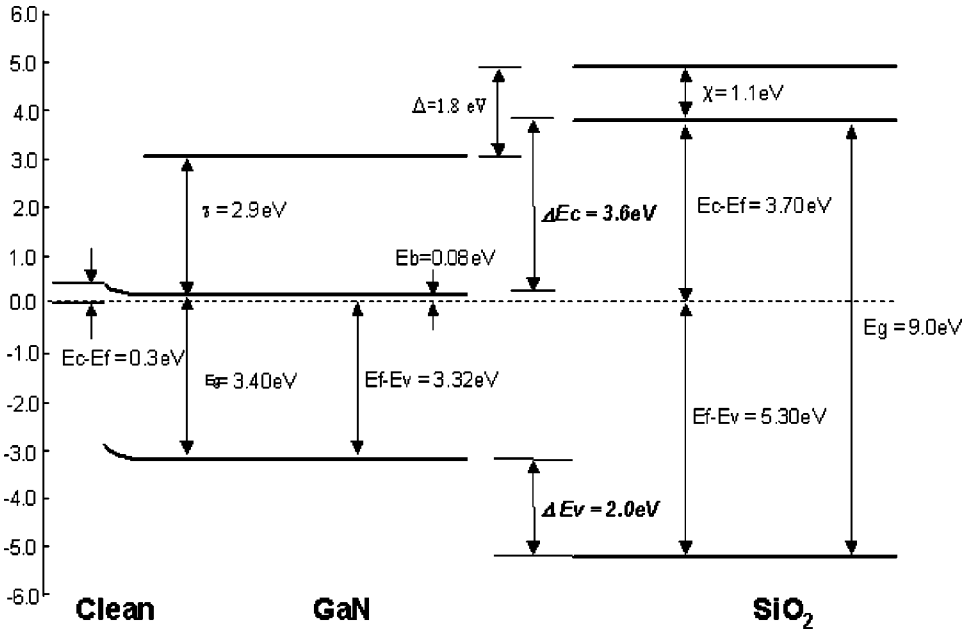

FIG. 9. Deduced bands for the clean *n*-type GaN surface (left) and the interface between *n*-type GaN and SiO_2. The valence band offset, conduction band offset, band bending, and interface dipole are represented.

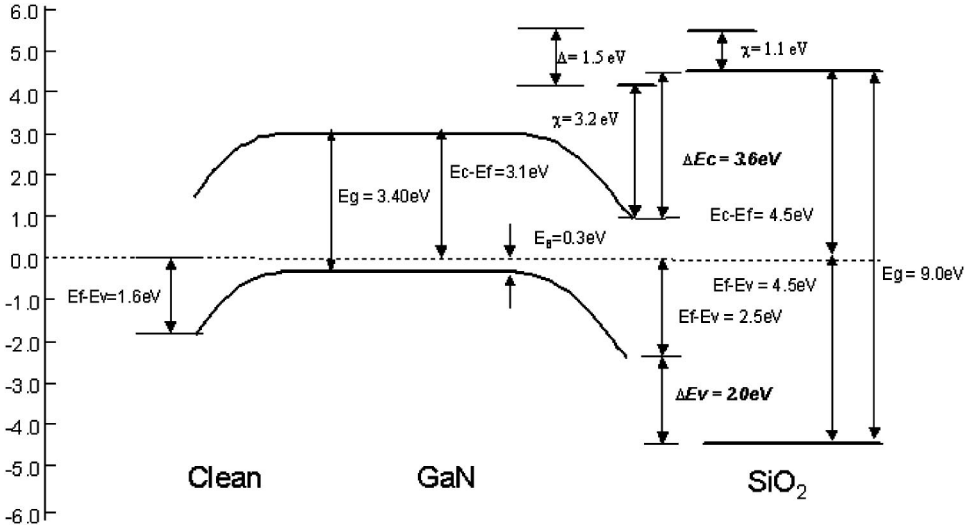

FIG. 10. Deduced bands for the clean *p*-type GaN surface (left) and the interface between *p*-type GaN and SiO_2. The valence band offset, conduction band offset, band bending, and interface dipole are represented.

The electron affinity levels for GaN and SiO_2 are represented in Figs. 9 and 10. The electron affinity model of heterojunction formation predicts these levels to align at the interface. Our results show a deviation from the electron affinity model of 1.8 eV for the *n*-type GaN substrate and 1.5 eV for the *p*-type GaN substrate.

The electron affinity model is based on the premise that the interface is formed without disruption of the surface electronic states of either of the two materials. All reference is to the vacuum levels of the two materials. The measured difference between the prediction of the electron affinity model and the experimentally observed band offset represents a change in the interface dipole. In general, it is not possible to assign a specific interface dipole to the heterostructure, but it is reasonable to consider the change in interface dipole from that deduced by the electron affinity model. However, the relation to the vacuum level in the first place is somewhat arbitrary. While the electron affinity of a surface can be determined following the approach employed in this study, it is dependent on the details of the surface structure where surface reconstruction, steps, and adsorbates can cause changes of the electron affinity by several eV. Moreover, after interface formation, the vacuum level of the materials at the interface is not defined or measurable, and the interface structure may have little relation to the specific bonding of the free surface that was responsible for the value of the electron affinity.

As an alternative to the electron affinity model, it has been proposed that heterojunction band alignments are determined by alignment of the charge neutrality levels of the two materials. The charge neutrality levels represent the branch point of the surface or interface states related to the valence or conduction band. Thus a neutral interface would have a Fermi level at the branch point. The presumption is that charge can transfer between the interface states of the two materials, which will cause an interface dipole. If the density of states is high or if the CNL's of the two semiconductors are at similar relative energies, then the band offset will be determined by the relative position of the CNL's of the two materials.

Recently, Robertson[24] adapted the interface defect model presented by Cowley and Sze[52] to employ the CNL's as the pinning levels. The model was applied to analyze the band alignment of a range of oxides on silicon, and the model seems consistent with most experimental results. In this model, charge transfer across the interface creates a dipole, which modifies the band lineup given by the electron affinity rule and is described by the relation

$$\phi_{\mathrm{CBO}}=(\phi_{\mathrm{CNL},a}-\phi_{\mathrm{CNL},b})-(E_{g,a}-E_{g,b})+S\{(\chi_a-\chi_b)+(E_{g,a}-E_{g,b})-(\phi_{\mathrm{CNL},a}-\phi_{\mathrm{CNL},b})\}, \quad (2)$$

where ϕ_{CBO} is the conduction band offset, χ and ϕ_{CNL} are the electron affinities and charge neutrality levels for each semiconductor (*a* and *b*), and *S* is a pinning factor based on the dielectric properties of the materials. Here, the ϕ_{CNL} are defined relative to the VBM of each semiconductor. A value of $S=1$ represents the EAM while a value of 0 represents pinning at the CN levels. To our knowledge, the CNL of SiO_2 has not been reported, and because of the high value of *S* for the SiO_2-Si interface (0.86),[24] we cannot use the experimental results of the Si/SiO_2 interface to reliably place the SiO_2 CNL.

In an attempt to understand the relation of our measured band alignment and the different models for heterostructure band alignment, we have compared our measured interface alignments to experimental results for SiO_2 on Si and SiO_2 on SiC in Fig. 11. In each case the diagrams are aligned to the vacuum level at the SiO_2 , which has been measured to be at the same energy relative to the oxide bands. The band gap of each material is indicated, as is the VBO. The position of the vacuum level of the clean surface of the semiconductor is indicated, and the difference between these values and the surface vacuum level is the deviation from the EAM. This difference represents the change in the interface dipole, and was found to be 0.5, 1.1, and 1.6 eV for SiO_2 on Si, SiC, and GaN, respectively.

Also indicated in Fig. 11 are the CNL's of the semiconductors based on prior reports.[24,53] We find that the CNL's of Si and GaN are in relative alignment with respect to the SiO_2

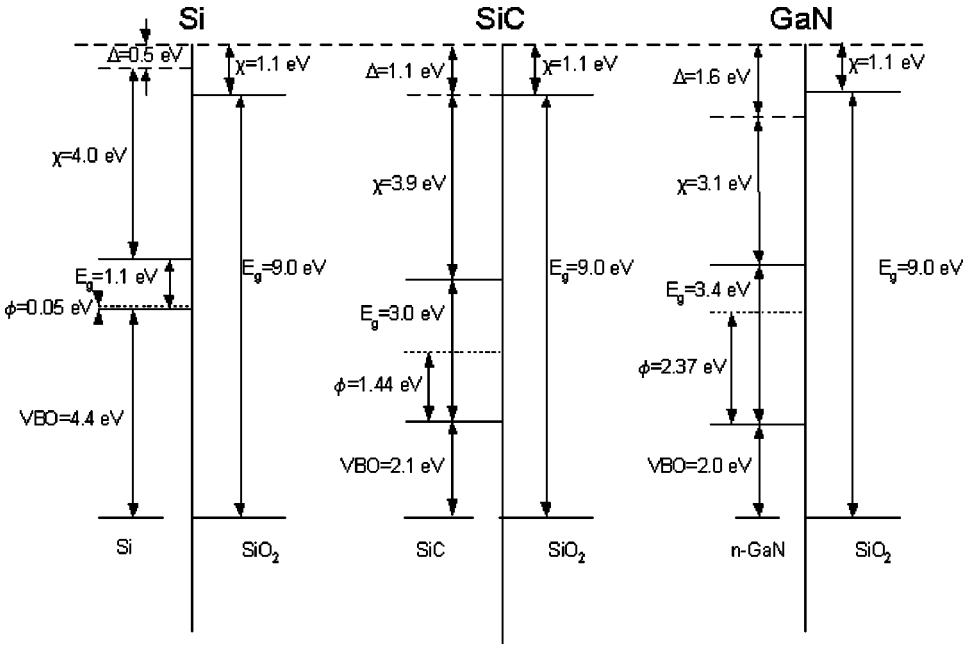

FIG. 11. Band alignment of Si/SiO_2, SiC/SiO_2, and GaN/SiO_2 interfaces. The dashed line at the top of the figure corresponds to the electron affinity of the SiO_2 surface, which is common in all three interfaces. The deviation from the electron affinity model is shown as Δ, and the charge neutrality level is indicated as a dashed line within the band gap. The VBO is determined from the measurements.

band gap, but the CNL of SiC falls substantially below these values. The variation of the CNL model for these three interfaces may be anticipated by the wide band gap and the high value of S of the SiO_2.

The progression of the interface dipole deduced from the deviation from the EAM is most likely related to the changes at the semiconductor surface since the oxide is the same in all cases. For the SiO_2/Si interface, the surface reconstruction of the Si is not expected to survive the bonding and this effect alone could account for the change in the interface dipole. The same might be true for the SiO_2/SiC interface where the increased interface dipole could also represent the charge transfer from the Si to the nearest neighbor C atoms. For both Si and SiC, the oxide interface layer is expected to contain Si-O bonding. For the SiO_2 /GaN interface, Ga-O bonding is expected at the interface. With the Ga atomic layer more positive and the O layer more negative, the interface dipole would be expected to lower the GaN electronic levels with respect to the SiO_2 levels, which is consistent with our observations.

V. CONCLUSIONS

The band alignment of a SiO_2 layer on 1×10^{17} cm^{-3} n-type and 2×10^{18} cm^{-3} p-type GaN has been investigated. Annealing in ammonia at 860 °C provided atomically clean, stoichiometric GaN surfaces with 0.3 ± 0.1 eV upward band bending and 1.3 ± 0.1 eV downward band bending for the n- and p-type surfaces, respectively. The electron affinity for the clean n- and p-type GaN surfaces was measured to be 2.9 and 3.2 eV, respectively. After careful formation of the GaN-SiO_2 interface, flatbands were observed in the n-type experiment, while an additional 0.9 eV downward band bending was observed for the p-type experiment. For both measurements, a valence band offset of 2.0 ± 0.1 eV was obtained, while the conduction band offset was determined to be 3.6 ± 0.1 eV (assuming $E_{g\,SiO_2}=9.0$ eV). The interface dipole deduced from comparison with the electron affinity model was 1.8 and 1.5 eV for the n- and p-type surface, respectively.

ACKNOWLEDGMENTS

We gratefully acknowledge M. Park and B. J. Rodriguez for helpful discussions and Jennifer Huening for the Raman measurements. This research was supported by the Office of Naval Research (MURI Project No. N00014-98-1-0654) and the Air Force Office of Scientific Research (Grant No. F49620-00-1-0253.)

[1] A. Munoz, N. Chetty, and Richard M. Martin, Phys. Rev. B **41**, 2976 (1990).
[2] E. H. Hurt, Ted E. Cook, Jr., K. M. Tracy, R. F. Davis, G. Lucovsky, and R. J. Nemanich, in *GaN and Related Alloys*, edited by J. E. Northrup, J. Neugebauer, S. F. Chichibu, D. C. Look, and H. Riechert, MRS Symposium Proceedings No. 693 (Materials Research Society, Pittsburgh, 2002), p. I9.10.1.
[3] Z. A. Wienberg and A. Hartstein, J. Appl. Phys. **54**, 2517 (1983).
[4] F. J. Grunthaner and P. J. Grunthaner, Mater. Sci. Rep. **1**, 65 (1986).
[5] S. Horiguchi and H. Yoshino, J. Appl. Phys. **58**, 1597 (1985).
[6] D. Babic and E. H. Nicollian, J. Appl. Phys. **78**, 4516 (1995).
[7] H. Nohira and T. Hattori, Appl. Surf. Sci. **117/118**, 199 (1997).
[8] J. Baur, K. Maier, M. Kunzer, U. Kaufmann, and J. Schneider, Appl. Phys. Lett. **65**, 2211 (1994).
[9] Z. Sitar, M. J. Paisley, B. Yan, F. Davis, J. Ruan, and J. W. Choyke, Thin Solid Films **200**, 311 (1991).
[10] G. Martin, A. Botchkarev, A. Rockett, H. Morkoc, and A. Botchkarev, Appl. Phys. Lett. **68**, 2541 (1996).
[11] S. W. King, R. F. Davis, C. Ronning, M. C. Benjamin, and R. J. Nemanich, Appl. Phys. Lett. **86**, 4483 (1999).
[12] J. T. Torvik, M. Leksono, J. I. Pankove, B. Van Zeghbroeck, H. M. Ng, and T. D. Moustakas, Appl. Phys. Lett. **72**, 1371 (1998).
[13] V. M. Bermudez, J. Appl. Phys. **80**, 1190 (1996).
[14] S. W. King, J. P. Barnak, M. D. Bremser, K. M. Tracy, C. Ronning, R. F. Davis, and R. J. Nemanich, J. Appl. Phys. **84**, 5248 (1998).
[15] H. C. Casey, Jr., G. G. Fountain, R. G. Alley, B. P. Keller, and S. P. DenBaars, Appl. Phys. Lett. **68**, 1850 (1996).
[16] M. Sawada, T. Sawada, T. Yamagata, K. Imai, H. Kimura, M. Yoshino, K. Iizuka, and H. Tomozawa, J. Cryst. Growth **189/190**, 706 (1998).

[17] S. Arulkumaran, T. Egawa, H. Ishikawa, T. Jimbo, and M. Umeno, Appl. Phys. Lett. **73**, 809 (1998).
[18] T. Sawada, Y. Ito, K. Imai, K. Suzuki, H. Tomozawa, and S. Sakai, Appl. Surf. Sci. **159-160**, 449 (2000).
[19] P. J. Hartlieb, W. Platow, A. Roskowski, R. F. Davis, and R. J. Nemanich, J. Appl. Phys. **91**, 732 (2002).
[20] C. I. Wu and A. Kahn, J. Vac. Sci. Technol. B **16**, 2218 (1998).
[21] K. Shiojima, R. Sugahara, and S. Sakai, Appl. Phys. Lett. **74**, 1936 (1999).
[22] R. Schlaf, O. Lang, C. Pettenkofer, and W. Jaegermann, J. Appl. Phys. **85**, 2732 (1999).
[23] J. Tersoff, Phys. Rev. B **30**, 4874 (1984).
[24] J. Robertson, J. Vac. Sci. Technol. B **18**, 1785 (2000).
[25] J. R. Waldrop and R. W. Grant, Phys. Rev. Lett. **43**, 1686 (1979).
[26] K. Horn, Appl. Phys. A: Solids Surf. **51**, 289 (1990).
[27] D. W. Kim, J. C. Bae, W. J. Kim, H. K. Baik, J. M. Myoung, and S. M. Lee, J. Electron. Mater. **30**, 183 (2001).
[28] A. R. Smith, R. M. Feenstra, D. W. Greve, M. S. Shin, M. Skowronski, J. Neugebauer, and J. E. Northrup, Appl. Phys. Lett. **72**, 2114 (1998).
[29] C. Kisielowski, J. Kruger, S. Ruvimov, T. Suski, J. W. Auger III, E. Jones, Z. Liliental-Weber, M. Rubin, E. R. Weber, M. D. Bremser, and R. F. Davis, Phys. Rev. B **54**, 17745 (1996).
[30] V. Yu. Davydov, N. S. Averkiev, I. N. Goncharuk, D. K. Nelson, I. P. Nikitina, A. S. Polkovnikov, A. N. Smirnov, M. A. Jacobson, and O. K. Semchinova, J. Appl. Phys. **82**, 5097 (1997).
[31] B. L. Ward, J. D. Hartman, E. H. Hurt, K. M. Tracy, R. F. Davis, and R. J. Nemanich, J. Vac. Sci. Technol. B **18**, 2082 (2000).
[32] C. I. Wu and A. Kahn, Appl. Phys. Lett. **74**, 546 (1999).
[33] R. Y. Korotkov, J. M. Gregie, and B. W. Wessels, Appl. Phys. Lett. **80**, 1731 (2002).
[34] J. R. Waldrop and R. W. Grant, Appl. Phys. Lett. **68**, 2879 (1996).
[35] D. Briggs and M. P. Seah, *Practical Surface Analysis* (Wiley, Chichester, England, 1990).
[36] V. Papaefthimiou, A. Siokou, and S. Kennou, J. Appl. Phys. **91**, 4213 (2002).
[37] D. Briggs, *Surface Analysis of Polymers by XOS and Static SIMS* (Cambridge University Press, Cambridge, England, 1998).
[38] H. P. Bonzel, G. Pirug, and J. Verhasselt, Chem. Phys. Lett. **271**, 113 (1997).
[39] C. C. Fulton, G. Lucovsky, and R. J. Nemanich, J. Vac. Sci. Technol. B **20**, 1726 (2002).
[40] W. Kern, J. Electrochem. Soc. **116**, 251C (1969).
[41] W. A. Pliskin and P. P. Castrucci, Electrochem. Technol. **6**, 85 (1968).
[42] S. Rojas, L. Zanotti, A. Borghesi, A. Sassalla, and G. U. Pignatel, J. Vac. Sci. Technol. B **11**, 2081 (1993).
[43] E. A. Kraut, R. W. Grant, J. R. Waldrop, and S. P. Kowalczyk, in *Heterojunction Band Discontinuities: Physics and Device Applications*, edited by F. Capasso and G. Margaritondo (Elsevier, New York, 1987).
[44] R. Dimitrov, V. Tilak, W. Yeo, B. Green, H. Kim, J. Smart, E. Chumbes, J. R. Shealy, W. Schaff, L. F. Eastman, C. Miskys, O. Ambacher, and M. Stutzman, Solid-State Electron. **44**, 1361 (2000).
[45] R. Therrien, G. Lucovsky, and R. Davis, Appl. Surf. Sci. **166**, 513 (2000).
[46] A. Zoroddu, F. Bernardini, P. Ruggerone, and V. Fiorentini, Phys. Rev. B **64**, 045208 (2001).
[47] N. Binggeli, P. Ferrara, and A. Baldereschi, Phys. Rev. B **63**, 245306 (2001).
[48] S. M. Sze, *Physics of Semiconductor Devices* (Wiley-Interscience, New York, 1981).
[49] V. K. Adamchuk and V. V. Afanasev, Phys. Status Solidi A **132**, 371 (1992).
[50] S. Miyazaki, T. Tamura, M. Ogasawara, H. Itokawa, H. Murakami, and M. Hirose, Appl. Surf. Sci. **159-160**, 75 (2000).
[51] S. Strite and H. Morkoc, J. Vac. Sci. Technol. B **10**, 1237 (1992).
[52] A. W. Cowley and S. M. Sze, J. Appl. Phys. **36**, 3212 (1965).
[53] W. Monch, J. Appl. Phys. **80**, 5076 (1996).